

# Photoinduced Oxygen Transfer and Double-Linkage Isomerism in a *cis*-(NO)(NO<sub>2</sub>) Transition-Metal Complex by Photocrystallography, FT-IR Spectroscopy and DFT Calculations

Andrey Yu Kovalevsky,\*<sup>[a]</sup> Graham King,<sup>[a]</sup> Kimberly A. Bagley,<sup>[b]</sup> and Philip Coppens\*<sup>[a]</sup>

**Abstract:** Photocrystallographic experiments show that laser exposure of crystals of [Ru(bpy)<sub>2</sub>(NO)(NO<sub>2</sub>)](PF<sub>6</sub>)<sub>2</sub> at 90 K produces a double isonitrosyl–nitrito linkage isomer and provide the detailed geometry of the metastable species generated. The analysis indicates that the isomerization is accomplished through an intramolecular

redox reaction involving oxygen transfer from the nitro to the nitrosyl group. At 200 K only a single (nitrito) linkage isomer is formed with a *U*-shaped conformation of the nitrito group rather

than the *Z* conformation observed at 90 K. A mechanism for the isomerization is proposed based on the crystallographic results and FTIR data collected at low temperatures during the isomerization process. The study presents the first structural evidence for double linkage isomerization in transition-metal complexes.

**Keywords:** density functional calculations • energy transfer • ruthenium

## Introduction

Ambidentate ligands are “the schizophrenics of coordination chemistry”, as Burmeister called them about fifteen years ago.<sup>[1]</sup> Many of two (NO, CN<sup>-</sup> etc.), three (NO<sub>2</sub><sup>-</sup>, SO<sub>2</sub>, CO<sub>2</sub>, NCS<sup>-</sup>, NCO<sup>-</sup>, NCSe<sup>-</sup> etc.) and even four-atomic ligands (DMSO, SO<sub>3</sub><sup>2-</sup>, etc.; excluding hydrogen atoms) can have different modes of coordination to transition metals. Such linkage isomers can either be chemically synthesized or generated by light,<sup>[2]</sup> high temperature and/or electrochemically.<sup>[3]</sup> In this context the nitro–nitrito isomerism (M–NO<sub>2</sub> ⇌ M–ONO) in transition-metal complexes occupies a special place. More than a century ago Jørgensen<sup>[4]</sup> was the first to synthesize both nitro- (NO<sub>2</sub>) and nitrito- (ONO) isomers of the [Co<sup>III</sup>(NH<sub>3</sub>)<sub>5</sub>NO<sub>2</sub>]<sup>2+</sup> cation. Since then, it was

also known that the nitro species can be converted into the nitrito species by irradiation with sunlight. The first systematic study on the photochemical behavior of NO<sub>2</sub>-containing transition-metal complexes was done by Adell in 1955, who showed that the red compound obtained from [Co(NH<sub>3</sub>)<sub>5</sub>NO<sub>2</sub>]Cl<sub>2</sub> on prolonged exposure to sunlight is the *O*-bound nitrito isomer.<sup>[5]</sup> The result was later confirmed by Wendlandt and Woodlock<sup>[6]</sup> by using UV light for the illumination of the samples. IR measurements by Balzani et al. and Heyns and de Waal showed that the stretching bands of the *N*-bound NO<sub>2</sub>, located at ~1430 and 1315 cm<sup>-1</sup>, shift to ~1460 and ~1060 cm<sup>-1</sup>, respectively, on irradiation.<sup>[7]</sup> The new light-induced bands correspond to the *O*-bound NO<sub>2</sub> linkage isomer. However, the X-ray crystallography of the Co<sup>III</sup> complex remains controversial. According to the single crystal X-ray analysis<sup>[8]</sup> of a previously irradiated crystal of [Co<sup>III</sup>(NH<sub>3</sub>)<sub>5</sub>NO<sub>2</sub>]Cl<sub>2</sub>, the nitrito group in the linkage isomer is bent, with a Co–O–N bond angle of 143(4)°, and has a *Z*-shaped configuration. On the other hand, the 1994 X-ray powder diffraction experiment<sup>[9]</sup> on the sunlight-illuminated sample of [Co<sup>III</sup>(NH<sub>3</sub>)<sub>5</sub>NO<sub>2</sub>]Br<sub>2</sub> showed a perfectly linear Co–O–N arrangement, although the unit cells of the two samples are identical. No further structural analysis of the light-induced nitro–nitrito isomerism in metal complexes has been performed since.

In addition to the isomerization process, the NO<sub>2</sub> ligand is capable of transferring its oxygen atom intramolecularly. The light-induced conversion of *o*-nitrobenzaldehyde to *o*-nitrosobenzoic acid was reported as early as 1901.<sup>[10]</sup> In a

[a] Dr. A. Y. Kovalevsky, G. King, Prof. Dr. P. Coppens  
Chemistry Department  
State University of New York at Buffalo  
Buffalo, NY 14260 (USA)  
Fax: (+1) 716 645 6948  
E-mail: ayk@gsu.edu  
coppens@buffalo.edu

[b] K. A. Bagley  
Department of Chemistry, State University College of New York at Buffalo, Buffalo, NY 14222 (USA)

Supporting information for this article is available on the WWW under <http://www.chemeurj.org/> or from the author: Final positional parameters, isotropic temperature parameters, anisotropic displacement parameters, bond lengths and angles for the 90 and 200 K structures.

metalloorganic complex the transfer can occur to a ligand coordinated *cis* to the nitrito. If this ligand is carbon monoxide (CO), the product of the reaction is carbon dioxide (CO<sub>2</sub>), which readily dissociates from a metal center.<sup>[11]</sup> In the case of nitrosyl (NO) being in the *cis* position to NO<sub>2</sub>, the oxygen atom transfer reaction results in the interconversion of the nitrito and nitrosyl substituents. The oxidative capability of the NO<sub>2</sub> ligand has been used extensively in transition-metal complexes containing the nitrito ligand that are catalysts for the mild oxidation of organic molecules.<sup>[12]</sup>

The ligand-to-ligand oxygen transfer reaction in transition-metal complexes was first observed for the iron(II) complex *cis*-[Fe(S<sub>2</sub>CNMe<sub>2</sub>)(NO)(NO<sub>2</sub>)] by Ileperuma and Feltham.<sup>[13]</sup> In chloroform solution the isotopically labeled complex [Fe(S<sub>2</sub>CNMe<sub>2</sub>)(<sup>15</sup>NO)(NO<sub>2</sub>)] is spontaneously equilibrated with [Fe(S<sub>2</sub>CNMe<sub>2</sub>)(NO)(<sup>15</sup>NO<sub>2</sub>)]. Unlike the reaction involving carbon monoxide, the oxygen transfer in the iron compound has no net change in the free energy ( $\Delta G$ ), except for the scrambling of the <sup>15</sup>N isotope. Interestingly, Dubrawski and Feltham<sup>[14]</sup> later demonstrated that the analogous ruthenium(II) complex did not undergo exchange between the NO and NO<sub>2</sub> ligands even under reflux or irradiation conditions. The absence of the reaction was explained by the kinetic inactivity and stability of the {RuNO}<sup>6</sup> species, compared with the iron complex. The thermally-induced oxygen transfer reaction occurs in crystals of [CpCr(NO)<sub>2</sub>(<sup>15</sup>NO<sub>2</sub>)], which equilibrates with [CpCr(<sup>15</sup>NO)(NO)(NO<sub>2</sub>)] at 50 °C.<sup>[15]</sup> During the reaction the oxygen may either be transferred to the nitrosyl from the nitro isomer or from the nitrito isomer, which would be first thermally generated. In MeOH solution at 24 °C the ligands spontaneously interconvert, similar to the iron complex. However, there is no evidence that nitrito species of this compound are generated in the solid state.

Ooyama et al.<sup>[16]</sup> reported on the synthesis and electrochemically and thermally-induced nitro–nitrito linkage isomerizations of *cis*-[Ru<sup>II</sup>(bpy)<sub>2</sub>(NO)(NO<sub>2</sub>)](PF<sub>6</sub>)<sub>2</sub>, with NO acting as a spectator ligand. Both the nitro- and nitrito isomeric forms can be synthesized. According to the IR experiments, in the solid state at 60 °C the nitro form gives an equilibrium mixture of both nitro and nitrito isomers. In a second publication Ooyama et al. reported that on one-electron electrochemical reduction of *cis*-[Ru<sup>II</sup>(bpy)<sub>2</sub>(NO)(ONO)]<sup>2+</sup> in solution, the {RuNO}<sup>7</sup> species, [Ru(bpy)<sub>2</sub>(NO)(ONO)]<sup>+</sup>, is generated which can be converted into the nitro species by a one-electron oxidation.<sup>[17]</sup> The reduced {RuNO}<sup>7</sup> intermediate species is stable at low temperature (–40 °C). During the electrochemically-induced isomerization an oxygen atom is transferred, since equimolar amounts of the [Ru(bpy)<sub>2</sub>(<sup>15</sup>NO)(NO<sub>2</sub>)] and [Ru(bpy)<sub>2</sub>(NO)(<sup>15</sup>NO<sub>2</sub>)] isotopomers were isolated. It seems reasonable to assume that the {Ru(NO)}<sup>7</sup> species is responsible for and actually facilitates the oxygen transfer reaction. Surprisingly, no similar studies have been done using the nitro-isomer as a starting material.

The light-induced changes in sodium nitroprusside dihydrate (Na<sub>2</sub>[Fe(CN)<sub>5</sub>(NO)]·2H<sub>2</sub>O, or SNP, were discovered in

1977, as part of a Mössbauer spectroscopy study of optical dispersion in transparent molecular systems.<sup>[18]</sup> In the same year, but quite unrelated, Rest and co-workers observed light-induced absorption bands in the IR spectrum of [Ni(NO)(η<sup>5</sup>-Cp)].<sup>[19]</sup> Subsequent DSC studies of the thermal decay of the new states of SNP revealed not one, but at least two light-induced species,<sup>[20]</sup> which were initially described as long-lived excited states, but later identified as linkage isomers with respectively inverted and side-on conformations of the NO ligand.<sup>[21,22]</sup>

Earlier we discussed the possibility of double linkage isomerization occurring on irradiation of [(tpp)Fe(NO)(NO<sub>2</sub>)].<sup>[23]</sup> The results were based on the solid state (KBr pellets) FT-IR data collected for the <sup>15</sup>N-isotopically labeled samples. No photocrystallographic experiments could be carried out due to the poor transparency of the porphyrin crystals to the laser light.

We now report that on photochemically-induced oxygen transfer in crystals of *cis*-[Ru<sup>II</sup>(bpy)<sub>2</sub>(NO)(NO<sub>2</sub>)](PF<sub>6</sub>)<sub>2</sub> a double linkage isonitrosyl–nitrito isomer is formed and present crystallographic and infrared evidence for the oxygen transfer between the NO<sub>2</sub> and NO ligands at low temperature. A mechanism for the dual process of atom transfer and linkage isomerization is proposed. The experimental data are supported by the quantum-mechanical DFT calculations.

## Experimental Section

**Preparation of the ruthenium complex:** The precursor complex *cis*-[Ru(bpy)<sub>2</sub>(NO<sub>2</sub>)<sub>2</sub>] was synthesized by the known method of Godwin and Meyer.<sup>[24]</sup> It was subsequently converted into the desired product *cis*-[Ru<sup>II</sup>(bpy)<sub>2</sub>(NO)(NO<sub>2</sub>)](PF<sub>6</sub>)<sub>2</sub> (**1**) by HCl(aq) acid by using the procedure of Ooyama et al.<sup>[16]</sup> Crystals suitable for single crystal X-ray analysis were obtained from the reaction mixture upon standing in the dark for several days.

**Photocrystallography:** X-ray diffraction data on **1**·H<sub>2</sub>O were collected at 200(1) and 90(1) K using a Bruker APEXII CCD diffractometer installed at a rotating anode source (MoK<sub>α</sub> radiation) and equipped with an Oxford Cryosystems nitrogen gas-flow apparatus. The data were collected by the rotation method with 0.3° frame-width ( $\omega$  scan) and 10–40 s exposure time per frame. For each experiment four sets of data (600 frames in each set) were collected, nominally covering half of reciprocal space. The data were integrated, scaled, sorted, and averaged by using the Apex2 software package.<sup>[25]</sup> The structures were solved by the direct methods using SHELXTL NT version 6.12.<sup>[26]</sup>

Crystals were mounted on the diffractometer and cooled to 200 or 90 K in two separate experiments. Ground-state structures (“dark”) at both temperatures were first collected. The crystals were irradiated in situ with 458 nm light from an Ar<sup>+</sup> CW laser for 5 and 10 min, respectively. During exposure, the crystals were continuously rotated around the diffractometer’s  $\phi$  angle to maximize the uniformity of irradiation. At 200 K a crystal was illuminated in five steps of 1 min each, the  $\phi$  angle being rotated the full 360° at each step. Similarly, at 90 K a crystal was irradiated in two steps of 5 min each. The laser output power was reduced to approximately 70 and 100 mW for 200 and 90 K experiments, respectively, to minimize damage to the crystals. During irradiation the crystals darkened from orange to red, although the color of the crystal after irradiation at 90 K is deeper than of the crystal irradiated at 200 K. Further irradiation resulted in the breaking of the crystal and the appearance of powder diffraction lines. As the crystals of the complex easily deteriorate

in laser light, the “dark” and “light” (after irradiation) data were collected on different crystals. Identical collection and integration procedures were used. Crystallographic data for **1**·H<sub>2</sub>O at 90 and 200 K are presented in Table 1.

Table 1. Crystallographic data for **1**·H<sub>2</sub>O at 90(1) K and 200(1) K.

	90(1) K		200(1) K	
	GS	MS	GS	MS
crystal color	orange	deep red	orange	red
shape	parallelepipeds	parallelepipeds	parallelepipeds	parallelepipeds
crystal system	monoclinic	monoclinic	monoclinic	monoclinic
space group	<i>P</i> <sub>2</sub> / <i>c</i>			
<i>a</i> [Å]	13.2704(4)	13.2690(5)	13.2726(4)	13.2325(8)
<i>b</i> [Å]	16.5029(5)	16.5355(6)	16.6610(5)	16.6661(9)
<i>c</i> [Å]	12.4436(4)	12.4724(4)	12.4912(4)	12.5484(7)
$\alpha$ [°]	90	90	90	90
$\beta$ [°]	94.4660(1)	94.367(1)	94.710(1)	94.809(2)
$\gamma$ [°]	90	90	90	90
<i>V</i> [Å <sup>3</sup> ]	2716.9(2)	2728.6(2)	2752.9(2)	2757.6(3)
<i>Z</i>	4	4	4	4
$\rho_{\text{calcd}}$ [g cm <sup>-3</sup> ]	1.950	1.941	1.924	1.921
$\mu$ [mm <sup>-1</sup> ]	0.820	0.816	0.809	0.807
max $2\theta$ [°]	63.42	60.06	69.34	59.82
absorption correction method	SADABS 2.10 <sup>[21]</sup>	SADABS 2.10 <sup>[21]</sup>	SADABS 2.10 <sup>[21]</sup>	SADABS 2.10 <sup>[21]</sup>
refls measd	58707	48785	59517	23691
unique refls ( <i>R</i> <sub>int</sub> )	11131 (0.034)	7967 (0.036)	11198 (0.036)	7840 (0.036)
refls <i>I</i> > 2 $\sigma$ ( <i>I</i> )	8857	6700	8229	5315
<i>R</i> <sub>1</sub> [ <i>I</i> > 2 $\sigma$ ( <i>I</i> )]	0.028	0.032	0.038	0.051
<i>wR</i> <sub>2</sub>	0.070	0.089	0.116	0.160
GOF	1.075	1.051	1.098	1.077

**FT-IR Measurements:** FT-IR experiments were performed on a BioRad FTS40 A IR spectrometer equipped with an MCT detector. An APD Helitran LT-3-110 optical cryostat equipped with NaCl windows and connected to a liquid nitrogen tank was used to cool the samples down to 90 K. Freshly prepared KBr pellets (approximately 1 mm thick) were mounted in an IR transmission cell. The cell was mounted in the cryostat and evacuated to approximately 10<sup>-7</sup> bar by using a turbo-molecular pump. The temperature of the sample was controlled to within 1 K using a Scientific Instruments temperature controller (9620-R-1-1). The sample was irradiated in situ at 200 or at 90 K for approximately 15–20 min with light from a 300 W Xe arc lamp passed through a heat absorbing water filter and a 300–500 nm broadband filter. Samples were mounted at 45° to both the IR beam and the irradiating light. Spectral resolution was 1 cm<sup>-1</sup>.

**Theoretical calculations:** All calculations were performed with the GAUSSIAN03 package<sup>[27]</sup> by using density functional theory (DFT) with the local density approximation (LDA) in the parametrization of Vosko, Wilk, and Nusair (SVWN5).<sup>[28]</sup> The effective core potential (ECP) LANL2DZ set was used for the ruthenium atom. A triple- $\zeta$  6-311G\*\* basis set was used for C, N, O and H atoms. All molecular geometries were optimized without symmetry restrictions. No imaginary frequencies were found. Convergence criteria of 10<sup>-6</sup> au for the density matrix, 4.5 × 10<sup>-4</sup> au Å<sup>-1</sup> for the gradients, and 1.8 × 10<sup>-3</sup> Å for the displacements were used. All calculations were spin-restricted.

## Results

**Ground-state structure:** The crystallographic data for compound **1**·H<sub>2</sub>O were collected at 90 and 200 K, whereas the previously published data<sup>[16]</sup> were collected at room temperature. The structures were refined by full-matrix least-squares with anisotropic temperature parameters for all

non-hydrogen atoms. Hydrogen atoms were located in the difference Fourier maps and subsequently refined using the “riding” model with  $U_{\text{iso}} = 1.2U_{\text{eq}}$  of the connected carbon atom. The hydrogen atoms on the solvent water molecule were refined independently with  $U_{\text{iso}} = 1.2U_{\text{eq}}$  of the oxygen atom. Final agreement factors are  $R_1 = 0.028$ ,  $wR_2 = 0.070$  (90 K), and  $R_1 = 0.038$ ,  $wR_2 = 0.116$  (200 K). Final positional, isotropic temperature parameters and anisotropic displacement parameters are listed in Tables S1 and S2 for the 90 K data and in Tables S4 and S5 for the 200 K data (see Supporting Information), while bond lengths and angles are given in Table S3 (90 K) and Table S6 (200 K). The molecular structure at 90 K is illustrated in Figure 1.

**The structures of the metastable species:** The refinement

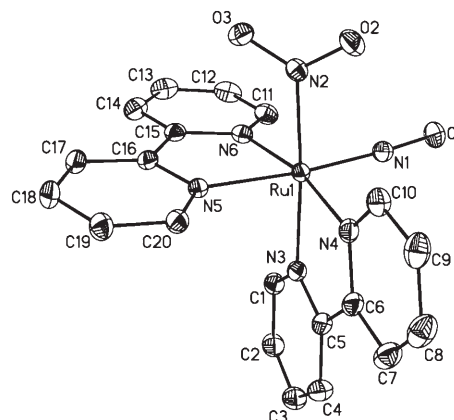


Figure 1. Geometry of the cation of **1** and numbering of the atoms (90 K). 50% probability ellipsoids are shown. H-atoms are omitted for clarity. The geometry at 200 K is essentially identical.

procedure has been previously described in the analysis of the metastable state MS2 structures of ruthenium sulfur dioxide complexes<sup>[24,29]</sup> and of iron nitrosyl linkage isomers. It was followed exactly, except that the bipyridine ligands were constrained to their ground-state geometries from the 90 and 200 K experiments.

Refinement of only the scale factor by using the ground-state (GS) molecule geometry yielded the agreement factors  $R_1 = 0.077$ ,  $wR_2 = 0.250$  (90 K) and  $R_1 = 0.098$ ,  $wR_2 = 0.269$  (200 K). The photodifference maps using the scale factors from the two refinements (Figures 2 and 3) showed several

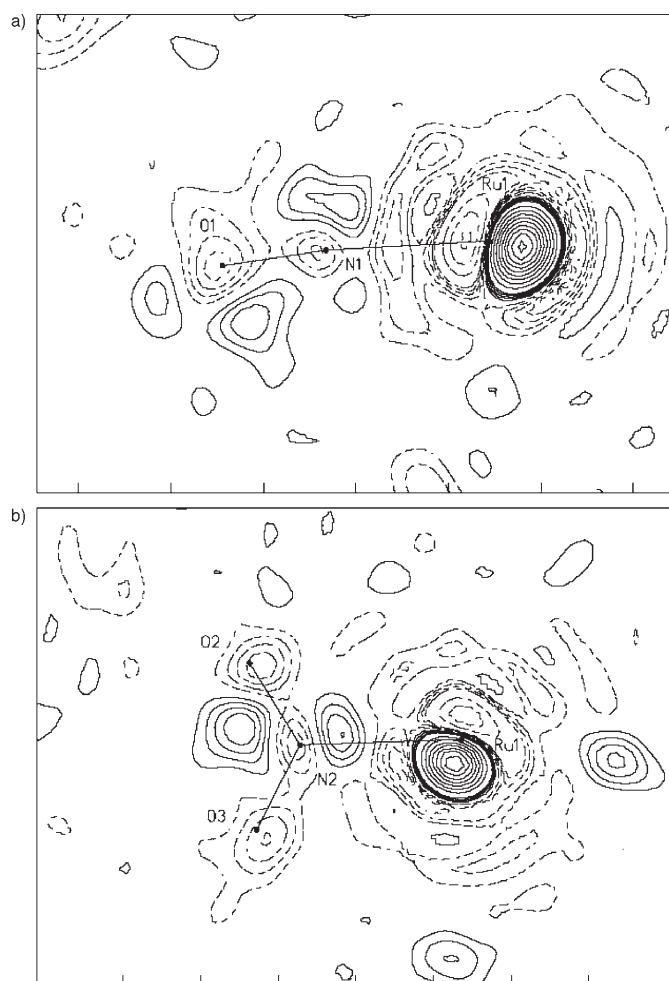


Figure 2. Photodifference Fourier maps of  $1\cdot\text{H}_2\text{O}$  at 90 K: a) in the plane containing Ru and NO ligand; b) in the plane containing Ru and  $\text{NO}_2$  ligand. Contours are at an  $0.2 \text{ e}\text{\AA}^{-3}$  interval up to  $1.0 \text{ e}\text{\AA}^{-3}$ , above which the interval is  $1.0 \text{ e}\text{\AA}^{-3}$ .

light-induced residual features, ranging from a maximum of  $11.5$  to a minimum of  $-3.05 \text{ e}\text{\AA}^{-3}$ ,  $0.37$  and  $0.26 \text{ \AA}$  from the position of the ground-state ruthenium atom, respectively, in the 90 K data; and a maximum of  $6.73$  and a minimum of  $-2.75 \text{ e}\text{\AA}^{-3}$ ,  $0.41$  and  $0.24 \text{ \AA}$  from the position of the ground-state ruthenium atom, respectively, in the 200 K data. Similar but smaller features were found near the light atoms of the cations. The pattern of light-induced peaks is in agreement with the  $\eta^1\text{-NO}_2$  (nitro) to  $\eta^1\text{-ONO}$  (nitrito) linkage isomerization. A nitrosyl–isonitrosyl isomerization of the NO ligand was found only in the 90 K data and unambiguously verified by anisotropic refinement of the atomic displacement parameters (ADP) of the NO ligand atoms. Unlike the nitrosyl model, refinement based on isonitrosyl gave physically meaningful ADPs (Figure 6, further discussed below). Most interestingly, the nitrito group appears at the former position of the nitrosyl ligand, while the (iso)nitrosyl group occupies the position formerly occupied by  $\text{NO}_2$ .

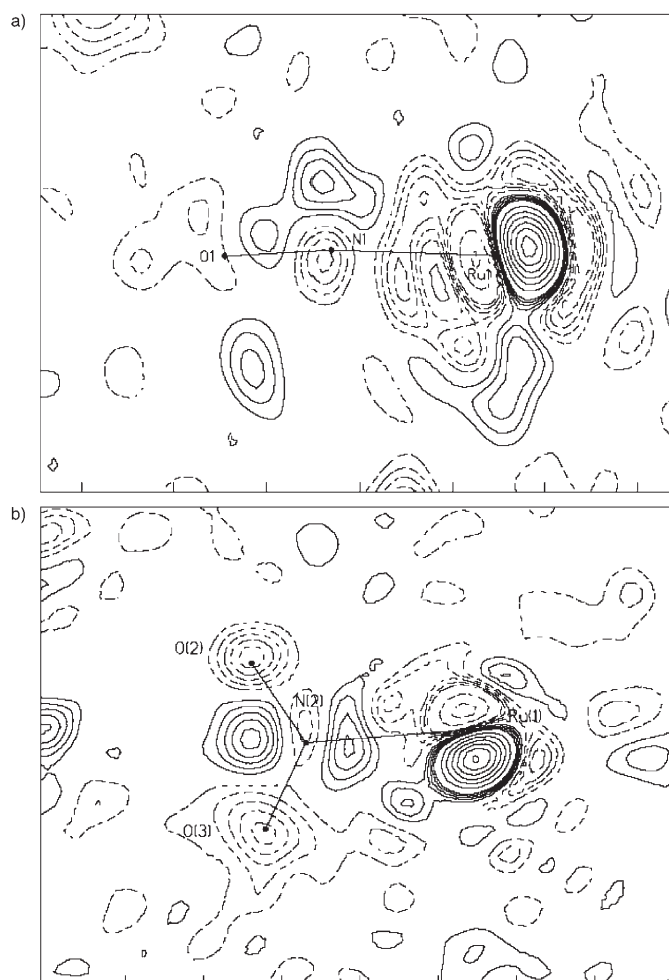


Figure 3. Photodifference Fourier maps of  $1\cdot\text{H}_2\text{O}$  at 200 K: a) in the plane containing Ru and NO ligand; b) in the plane containing Ru and  $\text{NO}_2$  ligand. Contours are at an  $0.2 \text{ e}\text{\AA}^{-3}$  interval up to  $1.0 \text{ e}\text{\AA}^{-3}$ , above which the interval is  $1.0 \text{ e}\text{\AA}^{-3}$ .

During the multi-step refinement procedure the anions and the solvent water molecule were fully refined. The population of the metastable states and their atomic coordinates were refined starting with the coordinates deduced from the photodifference maps. Isotropic parameters of the metastable state atoms were kept equal to the corresponding  $U_{\text{eq}}$  values of GS. The populations of the light-induced species were refined to  $9.1(1)$  and  $11.6(2)\%$  for the 90 and 200 K experiments, respectively. Subsequently, the GS was refined as a rigid body with all possible translations and rotations. In the final stage positional and isotropic thermal parameters (anisotropic for Ru and NO ligand) were also refined to give  $R_1=0.032$ ,  $wR_2=0.089$  (90 K), and  $R_1=0.051$ ,  $wR_2=0.160$  (200 K). The highest remaining maximum and deepest minimum in the difference Fourier synthesis were  $0.61$  and  $-1.33 \text{ e}\text{\AA}^{-3}$ , respectively, for the 90 K data; and  $1.11$  and  $-0.73 \text{ e}\text{\AA}^{-3}$ , respectively, for the 200 K data. Final positional and thermal parameters of the metastable state structures are listed in Table S7 (90 K) and Table S9 (200 K). The bond lengths and angles of the metastable state structures

are given in Table S8 (90 K) and Table S10 (200 K). The geometries of the light-induced species are illustrated in Figure 4.

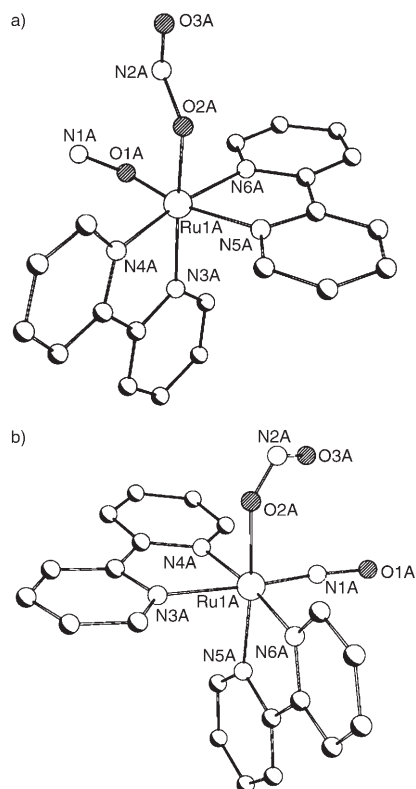


Figure 4. Geometry of the light-induced metastable states at a) 90 and b) 200 K.

**Infrared spectroscopy:** The IR spectra of *cis*-[Ru(bpy)<sub>2</sub>(NO)(ONO)](PF<sub>6</sub>)<sub>2</sub> are essentially the same as those reported by Ooyama and co-workers.<sup>[16]</sup> In the ground state the nitrosyl stretching band is located at 1943 and 1945 cm<sup>-1</sup> at 200 and 90 K, respectively. The asymmetric and symmetric NO<sub>2</sub> stretching vibrations are at 1430 and 1330 cm<sup>-1</sup>, respectively, at both temperatures. Photolysis at 200 K of the KBr pellets causes a sharp decrease of the intensity of the original bands, while the bands corresponding to the generation of MS<sub>200K</sub> appear at 1897 for the NO vibration, and 1495 and 983 cm<sup>-1</sup> for the nitrito stretching vibrations.  $\nu_{\text{NO}}$  is thus ~45 cm<sup>-1</sup> red-shifted in the metastable state, a value well in agreement with the theoretical results which show an NO downshift of 40 cm<sup>-1</sup> on nitro–nitrito isomerization. The shift may be explained by the increased electron density on the metal center compared with the GS and a corresponding increase in  $\pi$ -back donation. No other photoinduced IR bands are found in the spectra; therefore, the illumination at 200 K produces solely the mono-isomerized species characterized by the X-ray analysis.

The photoinduced IR spectrum at 90 K is more complex than that at the higher temperature (Figure 5). The ONO

bands are positioned similarly as in the 200 K spectra. A new band appears at 1815 cm<sup>-1</sup>, which was assigned to the isonitrosyl stretching vibration in accordance with previously published data.<sup>[23,30,34]</sup> After 5 min of irradiation only this band and the ONO vibrations are observable, with only very minor emergence of the 1892 cm<sup>-1</sup> band corresponding to the ONO-isomer-only species. On continued illumination of the sample the ON band's intensity increases only slightly, while the 1892 cm<sup>-1</sup> band noticeably builds up. When after 30 min of irradiation the sample is warmed to 160 K, the isonitrosyl band starts to decrease and virtually disappears after about 10 min. The intensity that is lost due to the isonitrosyl linkage isomer decay is returned to the 1892 cm<sup>-1</sup> band of the RuNO(ONO) metastable species and not to the original 1945 cm<sup>-1</sup> GS band of NO.

The evidence summarized above indicates that at 90 K the initial 5 min illumination produces the double linkage isomer (MS<sub>90K</sub>), in which both nitrosyl and nitro ligands are rearranged. The constancy of the 1815 cm<sup>-1</sup> band on further exposure implies that MS<sub>90K</sub> reaches its maximum concentration, while the nitrito mono-linkage isomer continues to increase. It likely has the same Z-shaped configuration of the ONO ligand as MS<sub>90K</sub>. Although no difference in the IR spectra was detected between the *U*- and *Z*-configurations of the nitrito group, the location of the nitrosyl band of the mono-isomerized cation at 1897 cm<sup>-1</sup> at 200 K and at 1892 cm<sup>-1</sup> at 90 K can be considered as another indication of different ONO configurations of the light-induced metastable states at different temperatures.

## Discussion

**Light-induced metastable states and oxygen atom transfer reaction:** Selected bond lengths and angles of the ground states and the metastable states at 90 and 200 K are compared in Tables 2 and 3, respectively.

Examination of the photodifference maps (Figures 2 and 3) clearly indicates the generation of light-induced species in the crystal at both 90 and 200 K. Negative difference electron density is observed at the positions of the ground-state atoms, while new peaks corresponding to the metastable states appear. It is clear that RuNO<sub>2</sub> → RuONO nitro–nitrito linkage isomerization occurs at both temperatures. However, the most striking feature in the photodifference maps is the location of the new light-induced peaks. The nitrito group appears at the position of the GS nitrosyl ligand site, and vice versa, the isonitrosyl (90 K) or nitrosyl (200 K) ligands are located at the sites of the GS nitro groups. Additionally, in the MS<sub>90K</sub> species the nitrito group has a *Z*-configuration, with its terminal NO bond pointing away from the center of the cation, whereas the nitrito group of the MS<sub>200K</sub> has a *U*-configuration, with its terminal NO bond *cis* to the Ru–O linkage (Figure 4).

Thus, in the metastable states at 90 and 200 K the NO<sub>2</sub> and NO ligands have switched places compared with their positions in the GS, pointing to an intramolecular oxygen

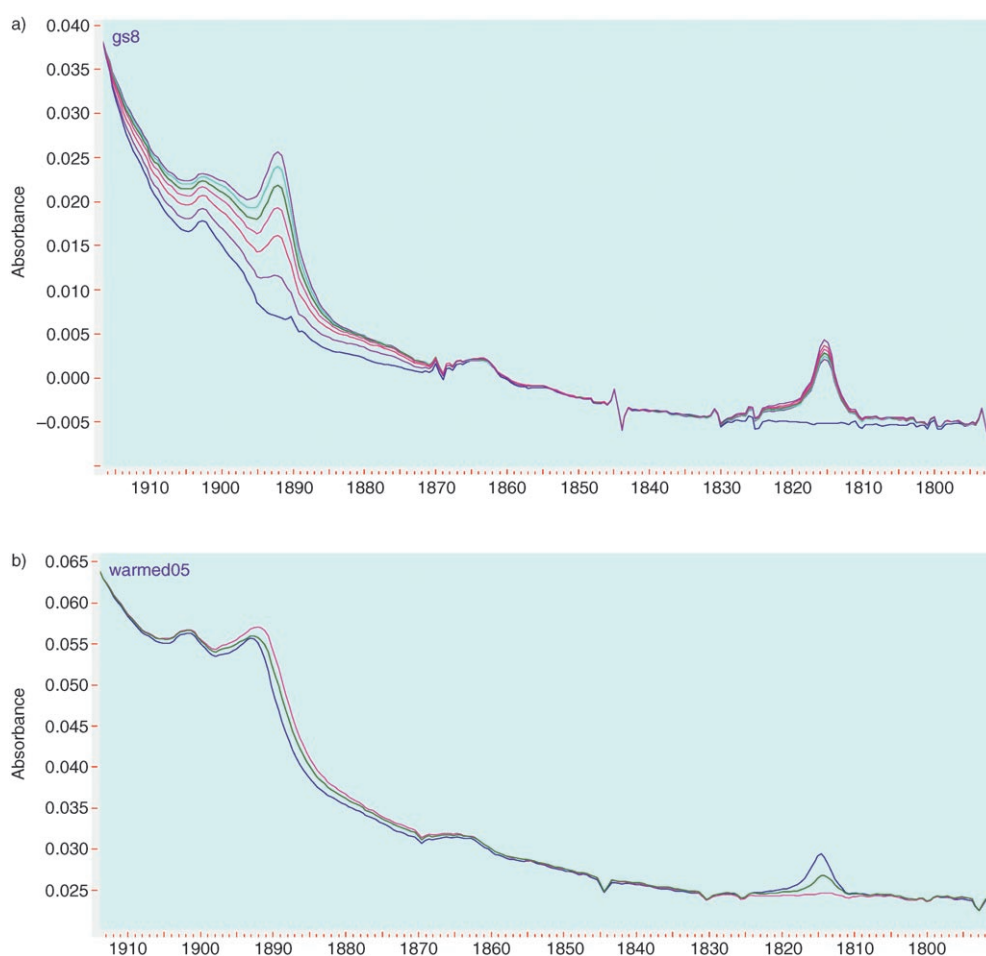


Figure 5. FT-IR spectra of the GS (blue curve) and irradiated sample (5 min steps) of  $[\text{Ru}(\text{bpy})_2(\text{NO})(\text{NO}_2)]$  at 90 K (a); warmed up to 160 K (5 min steps starting with the blue curve) after irradiation at 90 K (b). Frequencies in  $\text{cm}^{-1}$ .

Table 2. Selected experimental (90 K) and theoretical bond lengths [ $\text{\AA}$ ] and angles [ $^\circ$ ] for the *cis*- $[\text{Ru}(\text{bpy})_2(\text{NO})(\text{NO}_2)]^{2+}$  cation of **1**.

	Experiment		Theory	
	GS	MS <sub>90K</sub>	GS	MS <sub>90K</sub>
Ru1-N1	1.769(1)		1.778	
Ru1-N2	2.088(1)		2.105	
Ru1-O1		1.59(2)		1.908
Ru1-O2		2.02(2)		1.996
Ru1-N(bpy)	2.079(1)	2.055(8)	2.105	2.049
	2.079(1)	2.022(8)	2.083	2.012
	2.077(1)	2.088(8)	2.065	2.070
	2.072(1)	2.049(8)	2.060	2.048
N1-O1	1.130(2)	1.27(3)	1.138	1.142
N2-O2	1.236(1)	1.44(3)	1.218	1.363
N2-O3	1.232(2)	1.09(4)	1.211	1.174
N1-Ru1-N5	174.78(5)		170.0	
N2-Ru1-N3	174.01(4)		167.5	
N2-Ru1-N3	174.01(4)		167.5	
Ru1-N1-O1	174.5(1)		174.0	174
O1-Ru1-N5		168.0(9)		174.7
O2-Ru1-N3		166.8(7)		171.0
Ru1-O1-N1		168(2)		171.1
O2-N2-Ru1-N1	-43.9(1)		-50.5	
N2-O2-Ru1-O1		-24(2)		19.7

transfer reaction between the two groups on exposure to light. Such a reaction has not been reported before for this complex. Ooyama et al.<sup>[18]</sup> confirmed the transfer of an

Table 3. Selected experimental (200 K) and theoretical bond lengths [ $\text{\AA}$ ] and angles [ $^\circ$ ] for the *cis*- $[\text{Ru}(\text{bpy})_2(\text{NO})(\text{NO}_2)]^{2+}$  cation of **1**.

	Experiment		Theory	
	GS	MS <sub>200K</sub>	GS	MS <sub>200K</sub>
Ru1-N1	1.763(2)	1.68(2)	1.778	1.796
Ru1-N2	2.091(2)		2.105	
Ru1-O2		2.08(2)		2.051
Ru1-N(bpy)	2.079(2)	2.09(1)	2.105	2.074
	2.078(2)	2.07(1)	2.083	2.066
	2.077(2)	2.02(1)	2.065	2.063
	2.072(2)	2.01(1)	2.060	2.054
N1-O1	1.135(2)	1.18(3)	1.138	1.142
N2-O2	1.231(2)	1.10(3)	1.218	1.289
N2-O3	1.225(2)	1.41(4)	1.211	1.200
N1-Ru1-N5	174.69(7)		170.0	
N2-Ru1-N3	173.87(6)		167.5	
Ru1-N1-O1	174.8(2)	166(3)	174.0	166.5
N1-Ru1-N3		171(1)		173.5
O2-Ru1-N5		167.1(7)		168.7
O2-N2-Ru1-N1	-44.0(2)		-50.5	
N2-O2-Ru1-N1		21(3)		14.8

oxygen atom in the electrochemically reduced nitrosyl–nitrito species of the cation of **1**, as according to the IR spectroscopic measurements<sup>[18]</sup> mono-isotopically labeled Ru(NO)-(O<sup>15</sup>NO) or Ru(<sup>15</sup>NO)(ONO) are converted to Ru(<sup>15</sup>NO)-(<sup>15</sup>NO<sub>2</sub>). But the authors could not prove the existence of the reaction during the thermal linkage isomerization of the nitrosyl–nitro species, as the nitrito form is the only product of the reaction of the precursor *cis*-aquanitrosyl complex, which can be obtained as a <sup>15</sup>NO<sub>2</sub> labeled compound. The Ru(NO)(<sup>15</sup>NO<sub>2</sub>) or Ru(<sup>15</sup>NO)(NO<sub>2</sub>) complexes could not be synthesized.

It may be noted that the oxygen transfer reactions reported by Ooyama et al. and in this study do not take place spontaneously, unlike the intramolecular exchange in iron thiocarbamate compounds.<sup>[13]</sup> The generation of the ground-state Ru(NO)(NO<sub>2</sub>) species from the nitrito form and the formation of the nitrito form upon illumination of the GS nitro form are not followed by further chemical changes. If the light-induced metastable states were reactive and would undergo oxygen transfer in the reverse direction, the photodifference maps would contain the light-induced peaks corresponding to the nitrito ligand located at both the original sites of the nitrosyl and nitro groups. In fact, the photodifference maps at both 90 or at 200 K are unambiguous and provide evidence that the light-induced metastable species are the final products of the photo-process.

The identity of the NO ligand in the MS<sub>90K</sub> and MS<sub>200K</sub> is supported by anisotropic refinement of the displacement parameters of the nitrogen and oxygen atoms (Figure 6).

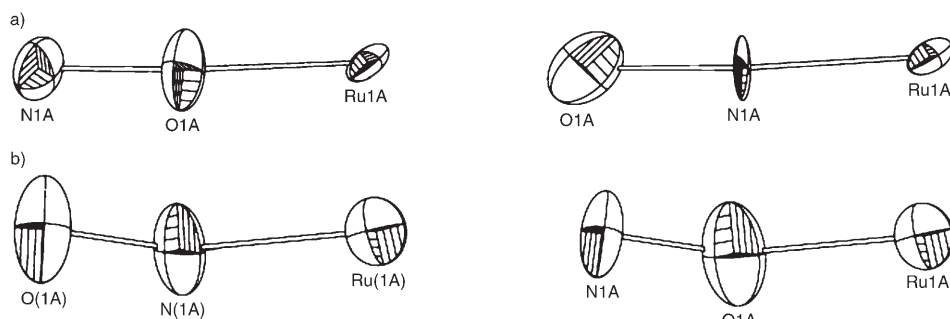


Figure 6. Thermal ellipsoids of the ruthenium–nitrosyl part of the cation in **1**·H<sub>2</sub>O. The Ru, N and O atoms are refined anisotropically assuming either the nitrosyl or isonitrosyl conformations. a) Evidence for isonitrosyl at 90 K; b) evidence for nitrosyl at 200 K.

In MS<sub>90K</sub>, physically acceptable thermal parameters are obtained only if the refinement is based on the isonitrosyl configuration. The displacement parameters of the nitrogen atom become too small and those of the oxygen too large when the RuNO arrangement is refined. The situation is reversed in the refinement of MS<sub>200K</sub>. The RuNO connectivity corresponds to reasonable displacement parameters for the two atoms, in contrast to the RuON configuration. The assignment of the nitrosyl versus isonitrosyl connectivity in the metastable states is in agreement with the FT-IR measurements.

**Effect of the transformation on the molecular interactions in the crystal:** In the ground state the O3 atom of the nitro group forms a weak C–H...O hydrogen bond with an aromatic hydrogen atom of one of the bipyridyl ligands (C14–H14A...O3' (1–x, 1–y, –z) 2.27 Å). This weak attractive interaction is lost during the photoreaction at 90 and 200 K.

In the crystal containing MS<sub>90K</sub> the terminal oxygen atom O3A of the photogenerated nitrito ligand has a shortened van der Waals contact with the aromatic carbon C7' (–x, y–0.5, 0.5–z) of 2.8 Å. No close contacts are formed in the crystal after the irradiation at 200 K. Thus the reaction cavity is only slightly perturbed during the photoreaction at 90, and not at all at 200 K. This is in agreement with our earlier studies on nitrosyl linkage isomerization, which show that such reactions typically occur within the space available in the crystal.<sup>[31]</sup>

**Geometry of the metastable states:** The structure of MS<sub>90K</sub> is the first X-ray crystallographic structure of a double linkage isomer of any transition-metal complex ever reported. The pseudo-octahedral environment of the ruthenium atom becomes even more distorted in the metastable state compared with the GS. The (N)O–Ru–N<sub>bpy</sub> and (ON)O–Ru–N<sub>bpy</sub> bond angles deviate by 12–13° from the ideal 180° values (Table 2). Furthermore, the isonitrosyl ligand is significantly bent, the N–O–Ru bond angle being as small as 168(2)°. The nitrogen atom of the ON ligand faces one of the bpy nitrogens and is displaced away from the ONO ligand. As calculated for the iron nitrosyl porphyrin complexes,<sup>[32]</sup> the Fe–N

distances located the direction of the ON tilt are shorter than the other Fe–N bonds. Such shortening was explained by Scheidt and Ellison<sup>[33]</sup> for {FeNO}<sup>7</sup> systems in terms of an increased d<sub>z<sup>2</sup></sub>–π\*(NO) interaction of a tilted d<sub>z<sup>2</sup></sub> orbital, and subsequent tilt and increased interaction with the basal σ orbitals leading to stronger Fe–N bonds. In the case of MS<sub>90K</sub> the ON is tilted along one of the Ru–N<sub>bpy</sub> bonds, which is 0.03 Å shorter than the average of the other distances to the bpy ligands (Table 2). The Ru–O distances to the isomerized ligands are shorter than the Ru–N bonds in the GS. This is in agreement with the geometry changes in the previously reported isonitrosyl<sup>[34]</sup> and nitrito structures,<sup>[16]</sup> and partly due to the stronger σ-donation of the electron-rich oxygen atom to the ruthenium. The N–O bond length of the isonitrosyl is lengthened as expected, although, the observed distance is at 1.27(3) Å longer than usually observed in metal–isonitrosyl light-induced complexes. Similarly, the N–O bond lengths in the ONO ligand are either longer (1.44(3) Å) or shorter (1.09(4) Å) than those usually obtained.<sup>[35]</sup> The large standard deviations, to

which the differences can be largely attributed, are due to the low (~10%) population of the MS<sub>90K</sub> state in the crystal. Nevertheless, the change in the NO distances upon formation of the nitrito group, such that the proximal N–O bond is longer than the terminal N–O bond, agrees well with the known structures containing the Z-shaped nitrito ligand bonded to ruthenium. Interestingly, the plane of the nitrito ligand makes a 24(2)° angle with the Ru–O bond of the isonitrosyl group, the angle being about 20° smaller than that of the nitro ligand in the GS. Such an orientation of ONO may have been preserved in the crystalline matrix after the oxygen transfer reaction, which would require a closer orientation of NO<sub>2</sub> towards NO than found in the GS (Table 2).

MS<sub>200K</sub> has a geometry similar to that of chemically synthesized *cis*-[Ru(bpy)<sub>2</sub>(NO)(ONO)]<sup>2+</sup> cation,<sup>[16]</sup> however, distinct differences are observed. Both structures have a U-shaped configuration of the nitrito ligand. The Ru–N(O) bond is slightly shorter than in the GS (Table 3). The Ru–O(NO) distance has not changed in MS<sub>200K</sub> with respect to the Ru–N bond length in the GS, whereas it shortened significantly in the chemically obtained nitrito complex.<sup>[16]</sup> The isonitrosyl ligand in MS<sub>90K</sub> and the nitrosyl ligand in MS<sub>200K</sub> are both significantly bent, but NO is almost linearly coordinated to Ru in the synthetic [Ru(bpy)<sub>2</sub>(NO)(ONO)]<sup>2+</sup> cation. In both MS<sub>90K</sub> and MS<sub>200K</sub> the tilt is along one of the Ru–N(bpy) bonds, the bond length being the shortest of the four Ru–N<sub>bpy</sub> bonds. Even though, the nitrosyl N–O bond is refined as longer in MS<sub>200K</sub> (1.18(3) Å) than in the GS, its distance is significantly shorter than that in the isonitrosyl in MS<sub>90K</sub> and is within 2σ from the GS value. On the other hand, in MS<sub>200K</sub> the N–O distances in the nitrito ligand are quite different from the values reported in the crystals of [Ru(bpy)<sub>2</sub>(NO)(ONO)]<sup>2+</sup>. The proximal N–O bond is significantly shortened compared with the terminal N–O bond, while the distances are reversed in the synthetic RuONO cation. As for MS<sub>90K</sub>, the low population of the MS<sub>200K</sub> (11.6(2)%) in the crystals prevents very accurate refinement of the positions of the light atoms.

**Theoretical calculations:** The calculations indicate that not only MS<sub>90K</sub> and MS<sub>200K</sub> but also other types of isomers correspond to local minima on the potential energy surface. They are schematically represented in Figure 7. The theoretical geometry of the GS is in a good agreement with the experimental geometry, the bond lengths being different by no more than 0.02 Å. The largest disagreement is for the nitro ligand, for which the calculation significantly underestimates the N–O distances. Interestingly, in the theoretical RuNO-(NO<sub>2</sub>) ground-state cation the pseudo-octahedral configuration of the central metal atom is greatly distorted, even to a greater extent than observed experimentally (Table 2). The N<sub>bpy</sub>-Ru–N(O) and N<sub>bpy</sub>-Ru–N(O<sub>2</sub>) bond angles are predicted to be 170 and 167.5°, respectively, about 4 and more than 6° below the observed values. On the other hand, the tilt of the NO ligand is well reproduced by the calculation (Table 2). According to the theory the plane of the NO<sub>2</sub> is almost stag-

gered with respect to the N<sub>bpy</sub>-Ru–N(O) moiety, the dihedral angle being ~50°, in good agreement with the experimental value.

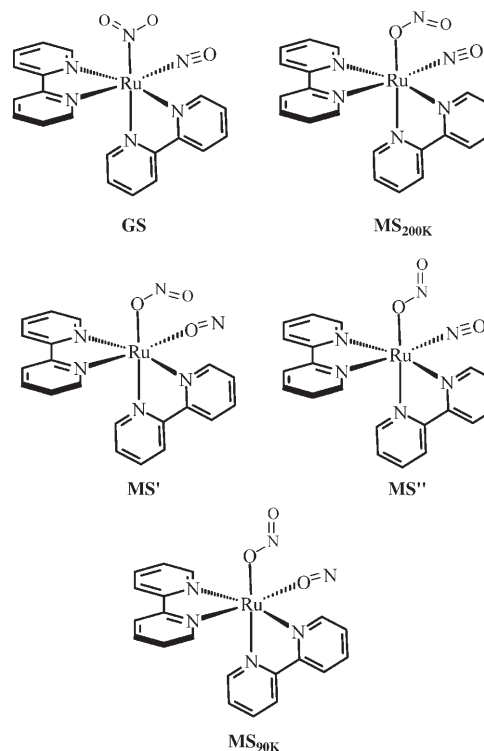


Figure 7. Chemical structures of the calculated metastable states.

MS<sub>200K</sub>, which has the U-shaped nitrito ligand and NO bonded as nitrosyl, is calculated to be energetically very slightly more stable (by 0.043 eV, 4.2 kJ mol<sup>-1</sup>) than the GS nitrosyl–nitro form and is thus as stable as the GS. This result is not unexpected, since both isomers can be prepared by wet chemistry methods.<sup>[16]</sup> The calculation reproduces the experimental geometry quite well, although the discrepancies in the bond lengths are larger than those for the GS geometry (Table 3), which may be attributed to the higher accuracy of the experimental geometry of the latter. However, the distortions around the ruthenium metal and the increased tilt of the NO ligand compared with the GS are in an excellent agreement with the experiment. NO is about 14° bent from the ideal linear geometry according to both experiment and calculation. Furthermore, the plane of the nitrito ligand is almost staggered with respect to the Ru–nitrosyl bond, the observed and the calculated values being 21(3) and ~15°, respectively. The change in the nitrito-ligand configuration from the U-form to the Z-form in MS'' (Figure 7) destabilizes the latter compared with both the GS and MS<sub>200K</sub>, its energy being 0.40 eV (38.1 kJ mol<sup>-1</sup>) higher than that of the GS, which explains why MS''<sub>Z</sub> was not detected in the experiments at 200 K.

As anticipated, the double linkage isomers have energies that are significantly higher than those of the single nitrito

linkage isomers (Figure 8). The double isomer MS', which has the more stable *U*-orientation of the ONO ligand but also the inverted NO ligand, is 1.86 eV (179.4 kJ mol<sup>-1</sup>) less

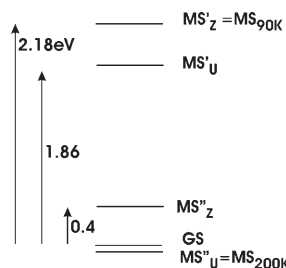


Figure 8. Calculated energy levels (eV) for the linkage isomers relative to the ground state (GS).

stable than the GS. The change of the ONO configuration to the *Z*-shape destabilizes the cation by an additional 0.32 eV. The observed Ru(ONO)(ON) MS<sub>90K</sub> isomer is 2.18 eV (210.2 kJ mol<sup>-1</sup>) higher in energy than the ground state. The difference between the MS' and MS'' configurations, corresponding to the effect of the NO isomerization, is calculated as 1.8–1.9 eV.

The calculated and observed geometry for MS<sub>90K</sub> and for MS<sub>200K</sub> are compared in Tables 2 and 3. In MS<sub>90K</sub> the O–N bond of the ONO ligand bonded to the Ru through the oxygen atom is calculated as much longer (1.363 Å) than the terminal bond (1.174 Å). The NO distance in the isonitrosyl ligand lengthens insignificantly, although the IR stretching frequency is shifted by about 130 cm<sup>-1</sup> relative to the GS NO stretching. The theoretical Ru–O(N) distance in the MS<sub>90K</sub> much longer than observed experimentally, and is quite elongated with respect to the Ru–N(O) bond length of the GS. The limited basis set used for the Ru atom may be the cause of these discrepancies. On the other hand, the experimental and theoretical distortions around the metal center and the isonitrosyl tilt are well reproduced. As in the MS<sub>200K</sub> isomer, the ONO ligand is rotated closer to the isonitrosyl ligand compared with the GS conformation of the nitro-ligand, the (O)N–O–Ru–O(N)

dihedral angle being 24(2) and ~20° according to experiment and calculation respectively (Table 2).

#### Mechanism of the photostimulated oxygen transfer reaction:

The proposed mechanism for the light-induced oxygen transfer reaction between the *cis* nitrosyl and nitro groups and the linkage isomerizations is presented schematically in Figure 9.

According to the theory the HOMO orbital is mostly localized on the 2p<sub>y</sub> atomic orbitals of NO<sub>2</sub> oxygen atoms, with a slight contribution from the atomic orbitals of the Ru and the NO<sub>2</sub> nitrogen (Figure 10a). In contrast, the LUMO orbital consists mainly of the 2p<sub>x</sub> orbitals of the NO ligand (Figure 10b). This orbital is essentially an antibonding π\* orbital of the nitrosyl, with some contribution from the Ru d<sub>xy</sub> atomic orbital. Therefore, the HOMO–LUMO excitation corresponds to a ligand-to-ligand charge transfer (LLCT), which simultaneously affects the nitro and the nitrosyl ligands.

For transition-metal nitrosyl compounds linkage isomerization occurs following the electron transfer from the metal to the NO π\* orbital (MLCT), leading after Renner–Teller distortion of the excited state to the formation of the η<sup>2</sup>-

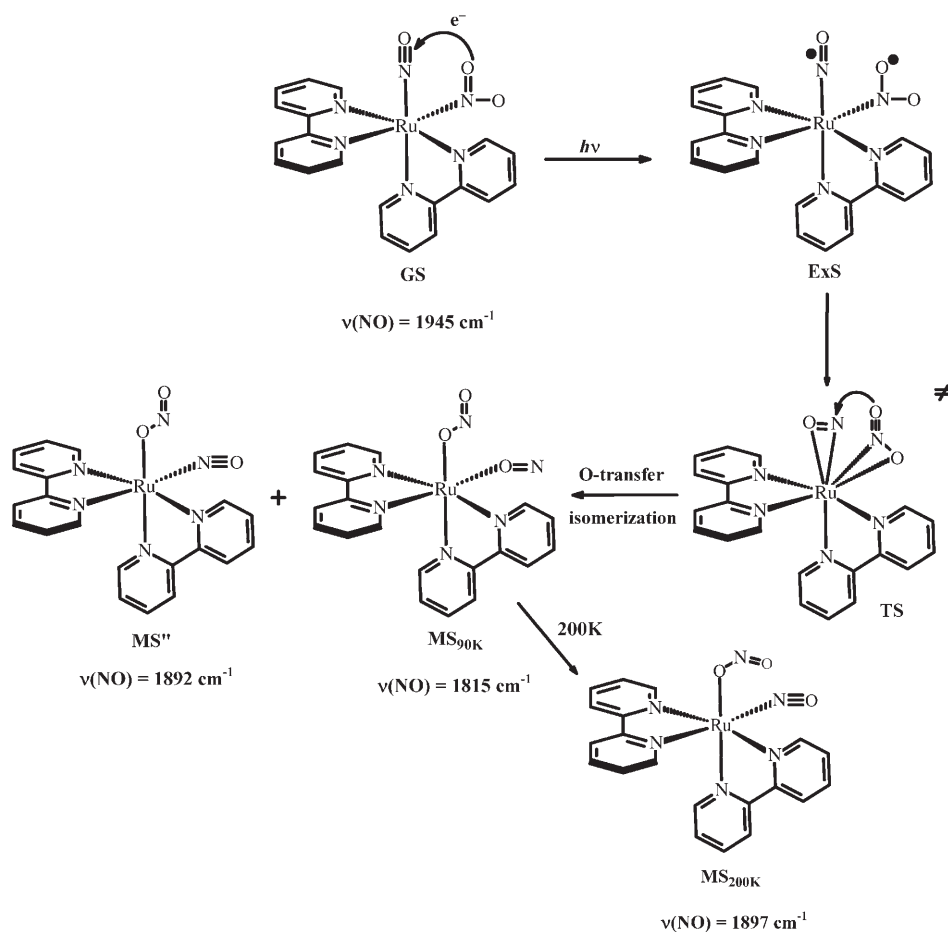


Figure 9. Proposed mechanism of the light-induced oxygen transfer reaction and the linkage isomerization. Stretching frequencies of the NO ligand are indicated.

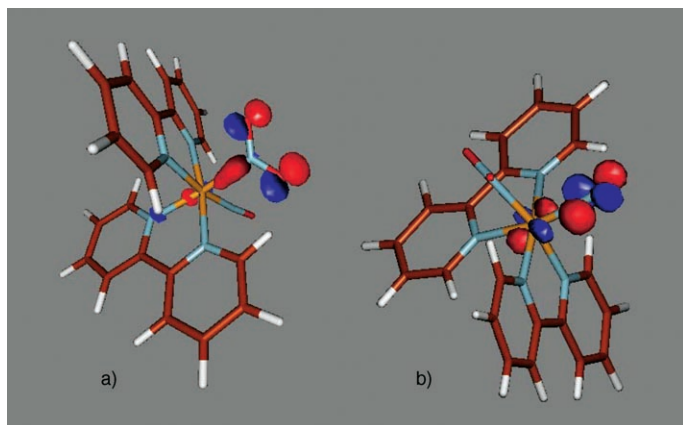


Figure 10. a) HOMO and b) LUMO of ground state of *cis*-[Ru(bpy)<sub>2</sub>(NO)(NO<sub>2</sub>)]<sup>2+</sup> cation. For the sake of clarity the HOMO and the LUMO are depicted in different molecular orientations.

side-on bound linkage isomer, which subsequently can be converted to the isonitrosyl species by absorption of an additional photon.<sup>[36]</sup> The  $\eta^2$ -NO is a metastable state, which has been previously detected and structurally characterized.<sup>[23]</sup> The mechanism of the NO<sub>2</sub> ligand isomerization involves the reverse process of an electron transfer from the nitro-group to the metal center (LMCT).<sup>[37]</sup> As proposed by Johnson and Pashman,<sup>[38]</sup> it is likely that the NO<sub>2</sub>→ONO isomerization reaction occurs through the  $\eta^2$ -side-on coordinated species, which is the putative transition state on the nitro-nitrito isomerization pathway (TS in Figure 9).

Given the composition of the LUMO of the [Ru(bpy)<sub>2</sub>(NO)(NO<sub>2</sub>)]<sup>2+</sup> cation, the HOMO–LUMO transition should lead to formation of a short-lived  $\eta^2$ -NO,  $\eta^2$ -NO<sub>2</sub>-ruthenium cation, and subsequent oxygen transfer and isomerization. According to this mechanism the eight-coordinated transition state relaxes into the MS<sub>90K</sub> metastable state by means of the oxygen transfer reaction and linkage isomerization in a concerted way. MS<sub>90K</sub> reaches an equilibrium concentration, as indicated by the rapid rise and subsequent constancy of the 1815 cm<sup>-1</sup> absorption feature (Figure 5), and then converts into MS' with an NO stretching frequency of 1892 cm<sup>-1</sup> (Figure 5), explaining the continued increase of the intensity of this band on continued irradiation. The assignment of the 1892 cm<sup>-1</sup> frequency to the NO in the nitrosyl–nitrito species is supported by the theoretical calculations, which predict a 40 cm<sup>-1</sup> downshift relative to the NO frequency in the parent species, which is observed at 1945 cm<sup>-1</sup>.

At 200 K MS'<sub>Z</sub> quickly relaxes to more stable MS<sub>200K</sub> with the U-shaped configuration of the nitrito group. The relaxation involves the rotation of the nitrito ligand around its proximal N–O bond, and does not require generation of the high-energy  $\eta^2$ -NO<sub>2</sub> coordinated species.

## Conclusion

We conclude that the double isonitrosyl–nitrito linkage isomerization that occurs on illumination of [Ru(bpy)<sub>2</sub>(NO)(NO<sub>2</sub>)](PF<sub>6</sub>)<sub>2</sub> at 90 K is accomplished through an intramolecular redox reaction involving oxygen transfer from the nitro to the nitrosyl group. At 200 K only a single (nitrito) linkage isomer is formed with a U-shaped configuration of the nitrito group rather than the Z-conformation observed at 90 K. The proposed mechanism is a one-photon process with a side-bound NO<sub>2</sub> transition state, as proposed earlier for nitro–nitrito isomerization. We note that the mechanism of formation of double linkage isomers in nitro–nitrosyl Fe porphyrins, for which evidence was found in our earlier IR studies,<sup>[24]</sup> should be different, as *trans*-substituents are involved in the latter case.

The existence of double-linkage isomerism, established in this study, further extends our knowledge of the binding of small molecule ligands to transition-metal atoms, a subject of key importance in many biological processes.

## Acknowledgements

Support of this work by the National Science Foundation (CHE0236317) is gratefully acknowledged.

- [1] J. L. Burmeister, *Coord. Chem. Rev.* **1990**, *105*, 77–133.
- [2] P. Coppens, I. Novozhilova, A. Kovalevsky, *Chem. Rev.* **2002**, *102*, 861–883 and references therein.
- [3] M. Sano, *Struct. Bonding (Berlin)* **2001**, *99*, 117–139; H. E. Toma, R. C. Rocha, *Croat. Chem. Acta* **2001**, *74*, 499–528.
- [4] S. M. Jørgensen, *Z. Anorg. Chem.* **1898**, *5*, 168–172.
- [5] B. Adell, *Z. Anorg. Allg. Chem.* **1955**, *279*, 219–224.
- [6] W. W. Wendlandt, J. H. Woodlock, *J. Inorg. Nucl. Chem.* **1965**, *27*, 259–260.
- [7] V. Balzani, R. Ballardini, N. Sabbatini, L. Moggi, *Inorg. Chem.* **1968**, *7*, 1398–1404; A. M. Heyns, D. de Waal, *Spectrochim. Acta* **1989**, *45*, 905–909.
- [8] M. Kubota, S. Ohba, *Acta Crystallogr. Sect. B* **1992**, *48*, 627–632.
- [9] N. Masciocchi, A. Kolyshev, V. Dulepov, E. Boldyreva, A. Sironi, *Inorg. Chem.* **1994**, *33*, 2579–2585.
- [10] G. Ciamician, P. Silber, *Chem. Ber.* **1901**, *34*, 2040–2046.
- [11] G. Booth, J. Chatt, *J. Chem. Soc.* **1962**, 2099–2102; W. Hieber, H. Z. Beutner, *Z. Anorg. Allg. Chem.* **1963**, *320*, 101–106; W. B. Hughes, *J. Chem. Soc. Chem. Commun.* **1969**, 1126–1127; K. R. Grundy, K. R. Laing, W. R. Roper, *J. Chem. Soc. Chem. Commun.* **1970**, 1500–1501; S. Bhaduri, B. F. G. Johnson, C. J. Savory, J. A. Segal, R. H. Walter, *J. Chem. Soc. Chem. Commun.* **1974**, 809–810; C. M. Gordon, R. D. Feltham, J. J. Turner, *J. Phys. Chem.* **1991**, *95*, 2889–2894.
- [12] See for example J. P. Solar, F. Mares, S. E. Diamond, *Catal. Rev. Sci. Eng.* **1985**, *27*, 1–28; M. A. Andrews, T. C. T. Chang, C. W. F. Cheng, *Organometallics* **1985**, *4*, 268–274; J. E. Bäckvall, A. Heumann, *J. Am. Chem. Soc.* **1986**, *108*, 7107–7108.
- [13] O. A. Ileperuma, R. D. Feltham, *J. Am. Chem. Soc.* **1976**, *98*, 6039–6040; O. A. Ileperuma, R. D. Feltham, *Inorg. Chem.* **1977**, *16*, 1876–1883.
- [14] J. V. Dubrawski, R. D. Feltham, *Inorg. Chem.* **1980**, *19*, 355–363.
- [15] J. L. Hubbard, C. R. Zoch, W. L. Elcesser, *Inorg. Chem.* **1993**, *32*, 3333–3338.

- [16] D. Ooyama, N. Nagao, H. Nagao, Y. Miura, A. Hasegawa, K.-I. Ando, F. S. Howell, M. Mukaida, K. Tanaka, *Inorg. Chem.* **1995**, *34*, 6024–6033.
- [17] D. Ooyama, N. Nagao, H. Nagao, F. C. Howell, M. Mukaida, *Chem. Lett.* **1996**, 759–760; D. Ooyama, H. Nagao, K. Ito, N. Nagao, F. C. Howell, M. Mukaida, *Bull. Chem. Soc. Jpn.* **1997**, *70*, 2141–2149.
- [18] U. Hauser, V. Oestreich, H. D. Rohrweck, *Z. Phys. A* **1977**, *280*, 17–25; U. Hauser, V. Oestreich, H. D. Rohrweck, *Z. Phys. A* **1977**, *280*, 125–130.
- [19] O. Crichton, A. J. Rest, *J. Chem. Soc. Dalton Trans.* **1977**, 986–993.
- [20] H. Zöllner, T. Woike, W. Krasser, S. Haussühl, *Z. Kristallogr.* **1989**, *188*, 139–153.
- [21] M. D. Carducci, M. R. Pressprich, P. Coppens, *J. Am. Chem. Soc.* **1997**, *119*, 2669–2678.
- [22] P. Coppens, D. V. Fomitchev, M. D. Carducci, K. Culp, *J. Chem. Soc. Dalton Trans.* **1998**, 865–872.
- [23] J. Lee, A. Yu. Kovalevsky, I. V. Novozhilova, K. A. Bagley, P. Coppens, G. B. Richter-Addo, *J. Am. Chem. Soc.* **2003**, *125*, 7180–7181.
- [24] J. B. Godwin, T. Meyer, *Inorg. Chem.* **1971**, *10*, 471–474.
- [25] Apex2, version 1.0–22 and SAINTPLUS, version 7.06, area detector control and integration software, Bruker AXS, Madison, WI, **2003**.
- [26] SHELXTL, version 6.12; integrated system for solving, refining and displaying crystal structures from diffraction data, Bruker AXS, Madison, WI, **2003**.
- [27] Gaussian 03, Revision A.1, M. J. Frisch, G. W. Trucks, H. B. Schlegel, G. E. Scuseria, M. A. Robb, J. R. Cheeseman, J. A. Montgomery, Jr., T. Vreven, K. N. Kudin, J. C. Burant, J. M. Millam, S. S. Iyengar, J. Tomasi, V. Barone, B. Mennucci, M. Cossi, G. Scalmani, N. Rega, G. A. Petersson, H. Nakatsuji, M. Hada, M. Ehara, K. Toyota, R. Fukuda, J. Hasegawa, M. Ishida, T. Nakajima, Y. Honda, O. Kitao, H. Nakai, M. Klene, X. Li, J. E. Knox, H. P. Hratchian, J. B. Cross, V. Bakken, C. Adamo, J. Jaramillo, R. Gomperts, R. E. Stratmann, O. Yazyev, A. J. Austin, R. Cammi, C. Pomelli, J. W. Ochterski, P. Y. Ayala, K. Morokuma, G. A. Voth, P. Salvador, J. J. Dannenberg, V. G. Zakrzewski, S. Dapprich, A. D. Daniels, M. C. Strain, O. Farkas, D. K. Malick, A. D. Rabuck, K. Raghavachari, J. B. Foresman, J. V. Ortiz, Q. Cui, A. G. Baboul, S. Clifford, J. Cioslowski, B. B. Stefanov, G. Liu, A. Liashenko, P. Piskorz, I. Komaromi, R. L. Martin, D. J. Fox, T. Keith, M. A. Al-Laham, C. Y. Peng, A. Nanayakkara, M. Challacombe, P. M. W. Gill, B. Johnson, W. Chen, M. W. Wong, C. Gonzalez, J. A. Pople, Gaussian, Inc., Pittsburgh PA, **2003**.
- [28] S. H. Vosko, L. Wilk, M. Nusair, *Can. J. Phys.* **1980**, *58*, 1200–1211.
- [29] A. Yu. Kovalevsky, K. A. Bagley, P. Coppens, *J. Am. Chem. Soc.* **2002**, *124*, 9241–9248; A. Yu. Kovalevsky, K. A. Bagley, J. M. Cole, P. Coppens, *Inorg. Chem.* **2003**, *42*, 140–147.
- [30] D. V. Fomitchev, *Study of Light-Induced Linkage Isomers in Transition Metal Nitrosyls*, PhD Dissertation, State University of New York at Buffalo, **1998**; D. V. Fomitchev, K. A. Bagley, P. Coppens, *J. Am. Chem. Soc.* **2000**, *122*, 532–538.
- [31] D. V. Fomitchev, I. Novozhilova, P. Coppens, *Tetrahedron* **2000**, *56*, 6813–6821.
- [32] I. V. Novozhilova, P. Coppens, unpublished results.
- [33] W. R. Scheidt, M. K. Ellison, *Acc. Chem. Res.* **1999**, *32*, 350–358.
- [34] D. V. Fomitchev, T. R. Furlani, P. Coppens, *Inorg. Chem.* **1998**, *37*, 1519–1526; D. V. Fomitchev, P. Coppens, *Comments Inorg. Chem.* **1999**, *21*, 131–148.
- [35] K. M. Miranda, X. Bu, I. Lorkovic, P. C. Ford, *Inorg. Chem.* **1997**, *36*, 4838–4844; C. F. Works, C. J. Jocher, G. D. Bart, X. Bu, P. C. Ford, *Inorg. Chem.* **2002**, *41*, 3728–3736.
- [36] B. Delley, J. Schefer, Th. Woike, *J. Chem. Phys.* **1997**, *107*, 10067–10074; M. Atanasov, T. Schönherr, *J. Mol. Struct.* **2002**, *592*, 79–93.
- [37] V. Balzani, R. Ballardini, N. Sabbatini, I. Moggi, *Inorg. Chem.* **1968**, *7*, 1398–1404.
- [38] D. A. Johnson, K. A. Pashman, *Inorg. Nucl. Chem. Lett.* **1975**, *11*, 23–28.

Received: June 7, 2005  
Published online: September 27, 2005